JOURNAL OF BONE AND MINERAL RESEARCH
Volume 20, Number 9, 2005
Published online on April 18, 2005; doi: 10.1359/JBMR.050406

Spontaneous Fractures in the Mouse Mutant *sfx* Are Caused by Deletion of the *Gulonolactone Oxidase* Gene, Causing Vitamin C Deficiency

Subburaman Mohan,[1,2,3,4] Anil Kapoor,[1] Anny Singgih,[1] Zhang Zhang,[1] Tim Taylor,[1] Hongrun Yu,[1] Robert B Chadwick,[1,2] Yoon-Suk Chung,[1] Leah Rae Donahue,[5] Clifford Rosen,[6] Grace C Crawford,[5] Jon Wergedal,[1,2] and David J Baylink[1,2,3]

ABSTRACT: Using a mouse mutant that fractures spontaneously and dies at a very young age, we identified that a deletion of the *GULO* gene, which is involved in the synthesis of vitamin C, is the cause of impaired osteoblast differentiation, reduced bone formation, and development of spontaneous fractures.

Introduction: A major public health problem worldwide, osteoporosis is a disease characterized by inadequate bone mass necessary for mechanical support, resulting in bone fracture. To identify the genetic basis for osteoporotic fractures, we used a mouse model that develops spontaneous fractures (*sfx*) at a very early age.
Materials and Methods: Skeletal phenotype of the *sfx* phenotype was evaluated by DXA using PIXImus instrumentation and by dynamic histomorphometry. The *sfx* gene was identified using various molecular genetic approaches, including fine mapping and sequencing of candidate genes, whole genome microarray, and PCR amplification of candidate genes using cDNA and genomic DNA as templates. Gene expression of selected candidate genes was performed using real-time PCR analysis. Osteoblast differentiation was measured by bone marrow stromal cell nodule assay.
Results: Femur and tibial BMD were reduced by 27% and 36%, respectively, in *sfx* mice at 5 weeks of age. Histomorphometric analyses of bones from *sfx* mice revealed that bone formation rate is reduced by >90% and is caused by impairment of differentiated functions of osteoblasts. The *sfx* gene was fine mapped to a 2 MB region containing ~30 genes in chromosome 14. By using various molecular genetic approaches, we identified that deletion of the g*ulonolactone oxidase* (*GULO*) gene, which is involved in the synthesis of ascorbic acid, is responsible for the *sfx* phenotype. We established that ascorbic acid deficiency caused by deletion of the *GULO* gene (38,146-bp region) contributes to fractures and premature death because the *sfx* phenotype can be corrected in vivo by treating *sfx* mice with ascorbic acid and because osteoblasts derived from *sfx* mice are only able to form mineralized nodules when treated with ascorbic acid. Treatment of bone marrow stromal cells derived from *sfx/sfx* mice in vitro with ascorbic acid increased expression levels of type I collagen, alkaline phosphatase, and osteocalcin several-fold.
Conclusion: The *sfx* is a mutation of the *GULO* gene, which leads to ascorbic acid deficiency, impaired osteoblast cell function, and fractures in affected mice. Based on these and other findings, we propose that ascorbic acid is essential for the maintenance of differentiated functions of osteoblasts and other cell types.
J Bone Miner Res 2005;20:1597–1610. Published online on April 18, 2005; doi: 10.1359/JBMR.050406

Key words: rodent, bone, gene/genetic research, linkage, osteoblasts, osteoporosis

INTRODUCTION

OSTEOPOROSIS IS A DISEASE characterized by a loss of bone mass and strength, often resulting in bone fractures (most frequently of the hip, spine, and forearm) from even minor trauma. Such osteoporotic fractures are a significant cause of disability. Hip fracture alone is associated with a 15–25% excess mortality rate in the first year after fracture.[1] In addition, the direct medical cost associated with managing bone fractures was estimated to be in excess of 13 billion dollars in the United States in 1995 alone.[2] As the size of the world's population ≥50 years of age increases during the next several decades, it is likely that both the direct and indirect costs of such fractures will increase as well.[3] Therefore, successful efforts to reduce the number of osteoporotic fractures would lead to considerable

The authors have no conflict of interest.

[1]Molecular Genetics Division, Musculoskeletal Disease Center, Jerry L. Pettis Memorial VA Medical Center, Loma Linda, California, USA; [2]Department of Medicine, Loma Linda University, Loma Linda, California, USA; [3]Department of Biochemistry, Loma Linda University, Loma Linda, California, USA; [4]Department of Physiology, Loma Linda University, Loma Linda, California, USA; [5]The Jackson Laboratory, Bar Harbor, Maine, USA; [6]St Joseph Hospital, Bangor, Maine, USA.

savings in health care costs as well as improved health both in the United States and abroad.

A hallmark of osteoporosis is spontaneous fracture, and one of the most significant determinants of spontaneous fracture is low BMD. In women, BMD after the menopause is determined first by a peak BMD achieved by the early 20s, and subsequently by a rate of BMD loss after menopause.[4] Because genetics plays a large role in the variation in peak BMD found in different individuals, studies in the field of bone research focus primarily on identifying those genes involved in determining peak BMD.[5] Despite the identification of several potential candidate genes that may play a role in the development of peak BMD, there remain large gaps in our understanding of the molecular genetic mechanisms involved in the pathogenesis of osteoporosis.

To identify candidate genes that may be important in the development of osteoporosis, we studied a mutant mouse that develops spontaneous fractures at the very early age of 5–7 weeks.[6] In previous studies, it was found that these mutant mice homozygous for the spontaneous fracture (gene symbol: *sfx*) gene mutation appeared phenotypically normal until they were weaned at 21 days of age. Shortly thereafter, these *sfx* mice developed a number of irregularities, including an inability to maintain their normal pubertal growth, manifestation of both skeletal and hematocrit abnormalities, development of fractures, and finally premature death at ~7–8 weeks of age.[6] Interestingly, many of the features of the *sfx* mouse resemble characteristics of scurvy syndrome.[7–10]

Mice normally synthesize their own ascorbic acid because of the presence of a key enzyme in ascorbic acid synthesis, l-gulono-lactone-γ-oxidase (GULO), that is present in the liver.[11–15] This enzyme catalyzes the terminal reaction converting l-gulono-γ-lactone to l-keto-gulono-γ-lactone, whereupon l-ascorbic acid is produced through isomerizations.[11–15] The GULO enzyme is found in the liver of higher vertebrate species (pigs, rats, mice) and in the kidney of lower vertebrate species (birds, turtles, and some fish), but not in humans, primates, or guinea pigs.[11–15] Because mice can synthesize ascorbic acid, it is not considered an essential dietary component for this species, and therefore vitamin C is not usually added to mouse chow. In contrast, humans depend entirely on dietary supplementation for their vitamin C.

The *sfx* gene, already known to be located in chromosome 14, has now been identified as gulonolactone oxidase (GULO), which is involved in the synthesis of ascorbic acid.[13,15] The findings of this study provide the first genetic evidence that ascorbic acid deficiency in *sfx* mice contributes to impaired bone formation and spontaneous fractures and that treatment of *sfx* mice with ascorbic acid reverses the mutant phenotype. Our findings also show that impairment in differentiation of osteoblasts contributes to bone formation deficiency in *sfx* mice and that in vitro treatment of bone marrow–derived stromal cells from *sfx* mice with ascorbic acid corrects the deficiency in osteoblast differentiation.

MATERIALS AND METHODS

Materials

α-MEM was purchased from Gibco (Invitrogen, Grand Island, NY, USA). Calf serum was purchased from Atlanta Biologicals (Norcross, GA, USA). DMEM was purchased from Cellgrow (Media Tech, Herndon, VA, USA). Tissue culture dishes were purchased from Corning (Corning, NY, USA). Ascorbic acid, ascorbic acid 2-phosphate, β-glycerophosphate, and alizarin red were purchased from Sigma Chemicals (St Louis, MO, USA). All other chemicals were purchased from Sigma Chemicals or Fisher Scientific (Tustin, CA, USA).

Mice

The *sfx* phenotype first appeared in a BALB/cBy inbred strain and was discovered in the mouse mutant resource of the Jackson Laboratory.[6] Breeding pairs of *sfx* mice were obtained from the Jackson Laboratory and bred to produce homozygous and corresponding control mice at the Jerry L. Pettis Memorial VA Medical Center animal facility. The animals were fed with either a Harlan Teklad S-2335 mouse breeder diet -7004 (during breeding) or with a Harlan Teklad 4% mouse/rat diet-7001 (Harlan, Indianapolis, IN, USA). Neither of these diets contains any vitamin C. The levels of calcium, phosphorous, magnesium, and vitamin D were 0.82%, 0.53%, 0.25%, and 2.98 IU/g in the 7004 breeder diet and 1.85%, 0.89%, 0.29%, and 5.05 IU/g in the 7001 maintenance diet, respectively. All of the procedures were approved by the Institutional Care and Use Committee of the Jerry L. Pettis Memorial VA Medical Center, Loma Linda, CA.

Bone densitometry by DXA

Total BMC, total body BMD, lean body mass, and percent fat were measured by DXA using the PIXImus instrument (Lunar Corp., Madison, WI, USA). Areal BMD (aBMD) of the femora, tibias, and spine were also measured using the PIXImus instrument. The precision for BMC and BMD was ±1% for repeat measurements of the same bones.[16]

Dynamic histomorphometry

Histomorphometry was performed on samples from mice at 5 weeks of age. Mice were injected with calcein (20 mg/kg body weight) 8 and 2 days before death for sample collection. The femora were defleshed and embedded in methylmethacrylate. Thick cross-sections (0.5 mm thickness) were cut from the midpoint of the shaft and processed as described.[17] All bone histomorphometric parameters were measured with the OsteoMeasure system equipped with a digitizing tablet (OsteoMetrics, Atlanta, GA, USA) and a color video camera (Sony Corp.) as described.[17] Histomorphometric indices were based on nomenclature recommended by the American Society of Bone and Mineral Research.[18]

Biochemical assays

Serum osteocalcin levels were measured using a radioimmunoassay (RIA) validated for measuring mouse osteocalcin.[19] The sensitivity of the assay is 0.5 ng/ml. The inter- and intra-assay CVs are <8%. Serum levels of ascorbic acid were determined using the Roche Diagnostic kit (Roche Diagnostics, Branchburg, NJ, USA).

Genotyping

Genomic DNA was isolated from tail clips using mouse DNAeasy kits (Qiagen, Valencia, CA, USA). DNA samples were quantified and quality determined by measuring their absorbance at 260 and 280 nm. Genotyping was performed using selected microsatellite markers in chromosome 14. PCR reactions and running conditions allowed multiplexing of three to four microsatellite markers in a single electrophoretic lane. The pooled products were analyzed for fragment size on an ABI Model 3100 DNA Analyzer, and GeneScan software was used to size alleles (Applied Biosystems, Foster City, CA, USA). Allele calls and edits were performed using Genotyper software (Applied Biosystems).

PCR amplification of genomic DNA from control and *sfx* mice with appropriate primer sets was carried out using standard procedures.

RNA extraction

The Qiagen lipid extraction kit was used to extract RNA from bones with the following modification. After the death of the mice, bones were transferred to liquid nitrogen immediately and stored at –80°C until RNA extraction. Bones were ground into a fine powder using mortar and pestle with liquid nitrogen, and extracted with 1 ml of Trizol. RNA was precipitated with chloroform, solubilized in ethanol, and purified according to the instructions provided in the Qiagen kit. RNA extraction from soft tissues was performed using standard procedures. Quality and quantity of RNA were analyzed using a Bio-analyzer (Agilent Technologies, Westlake Village, CA, USA) and a Nano-drop instrument (Ambion, Austin, TX, USA).

Microarray analysis

An aliquot of 500 ng total RNA extracted from bones of control and *sfx* mice was reverse transcribed using a low RNA amplification and labeling kit and hybridized to a 20,000 mouse development oligo microarray purchased from Agilent. After hybridization, the slide was washed, dried, and scanned using an Agilent scanner. The images were analyzed using Resolver software and signal data were output together with the Agilent probe name, GenBank identification number, and gene description to a Microsoft Excel data spreadsheet. Any significant differences in mRNA intensities were determined by comparing intensities of control and *sfx* groups by Student's *t*-test.

Real-time PCR

Quantitation of mRNA expression was carried out by the SYBR green method on a 7900 sequence detection system (ABI PRISM) as recommended by the manufacturer. The data were analyzed using SDS software version 2. Data normalization was accomplished using the endogenous control gene (peptidyl prolyl isomerase A [PPIA]). ΔCt values were determined (Ct value for the gene of interest minus Ct value for control gene), and comparisons of Ct values were used for relative quantitation of gene expression. The fold change between the control and experimental groups was calculated based on a $2^{-\Delta\Delta}$Ct formula. The formula and its derivations were obtained from the user guide of ABI Prism 7900 Sequence Detection System (Applied Biosystems).

Nodule assay

Bone marrow cells were expelled from the femoral diaphysis with α-MEM using a syringe fitted with a 23-G needle. Cell suspension was counted with a hemocytometer. Subsequently, the bone marrow cells were plated at a density of 7×10^6 cells/90-mm per plastic tissue culture dish in α-MEM containing 10% calf serum, 100 U/ml penicillin, and 100 μg/ml streptomycin. Culture media were changed every 2 days for 6 days and then switched to mineralization media by adding 50 μg/ml ascorbic acid and 10 mM β-glycerophosphate. Additional 300 μg/ml ascorbic acid 2-phosphate was added to some *sfx* cultures. One-half of the media was changed every 3 days for 30 days. The mineralized matrix was stained for calcium by alizarin red staining method as described.[20] Briefly, after 30 days, cells were washed with PBS, followed by fixation in ice cold 70% ethanol for at least 1 h. Ethanol was removed, and cells were rinsed with water and stained with 40 mM alizarin red (pH 4.2) for 10 minutes at room temperature. Stained cells were further processed by five rinses with water, followed by a 15-minute wash in PBS with rotation to reduce nonspecific alizarin red stain. The mineralized area was measured with the OsteoMeasure system equipped with a digitizing tablet and a color video camera, as previously described.

For gene expression studies, bone marrow cells derived from *sfx* mice were plated in DMEM, which contained no ascorbic acid, and treated with vehicle or long acting ascorbic acid 2-phosphate (300 μg/ml). At various times after treatment, RNA was extracted and used for real-time PCR analyses using primers designed according to the instructions provided by Applied Biosystems. Conditioned media samples were collected and used for measurement of osteocalcin levels as described[19]

Statistical analysis

Data are presented as means ± SD and analyzed by Student's *t*-test or ANOVA as appropriate. One- and two-way ANOVA tests were performed using STATISTICA software (Statsoft, Tulsa, OK, USA).

RESULTS

sfx phenotype manifests after weaning

To better characterize the age dependence of the *sfx* phenotype, we measured musculoskeletal parameters by DXA using PIXImus in *sfx*/*sfx* mice and corresponding littermate

Table 1. Age-Related Change in the Body Weight and Musculoskeletal Parameters in Control and *sfx* Mice

Parameter	21 days		28 days		35 days	
	+/?	*sfx/sfx*	+/?	*sfx/sfx*	+/?	*sfx/sfx*
Body weight (g)	10.9 ± 1.2	9.5 ± 1.0	15.9 ± 2.1	10.3 ± 1.8‡	18.6 ± 1.3	11.1 ± 1.3‡
Lean body mass (g)	8.3 ± 1.0	7.3 ± 0.7	12.9 ± 2.0	8.1 ± 1.0‡	15.6 ± 1.8	9.0 ± 1.4‡
Percent fat	16.5 ± 2.7	17.5 ± 4.7	14.5 ± 1.7	14.8 ± 1.4	13.8 ± 1.6	14.4 ± 1.8
Total BMC (mg)	106 ± 27	91 ± 30	197 ± 24	168 ± 27	240 ± 28	184 ± 18†
Total body BMD (mg/cm^2)	27.3 ± 1.2	25.7 ± 2.9	33.8 ± 2.0	31.2 ± 2.0	36.5 ± 2.0	32.4 ± 0.8†
Femur BMC (mg)	5.3 ± 0.5	5.5 ± 3.0	13.2 ± 4.0	8.2 ± 1.9*	14.8 ± 2.9	8.7 ± 1.7†
Femur BMD (mg/cm^2)	33.0 ± 4.0	32.8 ± 7.0	47.1 ± 4.0	35.9 ± 3.0‡	51.0 ± 3.0	37.7 ± 3.0‡
Tibia BMD (mg/cm^2)	ND	ND	ND	ND	44.6 ± 6.0	28.5 ± 9.0§
Spine BMD (mg/cm^2)	ND	ND	ND	ND	36.1 ± 1.0	34.3 ± 2.0

Values are mean ± SD of five to seven observations per group. Two-way ANOVA revealed significant ($p < 0.001$) strain and age effects for body weight, lean body mass, total BMC, total body BMD, femur BMC, and femur BMD.

ND, not determined.

* $p < 0.005$; † $p < 0.01$, ‡ $p < 0.001$ vs. +/? control mice by posthoc Neuman-Keuls test.

§ $p < 0.01$ vs. +/? control mice by Student's *t*-test.

control +/? mice longitudinally. Table 1 shows that neither body weight nor any of the musculoskeletal parameters measured were significantly different in the *sfx*/*sfx* mice compared with the +/? mice at 21 days of age. However, body weight, lean body mass, BMC, and BMD of the total body and the femur were significantly less in the *sfx*/*sfx* mice compared with the +/? mice at 28 days of age. By 35 days of age, both body weight and lean body mass (LBM) were nearly 50% lower in the *sfx*/*sfx* mice compared with the +/? mice. Total body BMC and femur BMC were reduced by 25% and 45%, respectively, in the *sfx*/*sfx* mice compared with the +/? mice (Table 1). Accordingly, total body BMD and femur BMD were 12% and 27% lower in the *sfx*/*sfx* mice compared with the +/? mice. Whereas BMD of the tibia was decreased by 36%, BMD of the lumbar vertebra was decreased by only 5% in the *sfx*/*sfx* mice compared with the +/? mice. The percent fat was not decreased in the *sfx*/*sfx* mice compared with the +/? mice. These data show that the phenotype of the *sfx* mouse manifests itself principally during the period between weaning and attainment of sexual maturity and that bone deficits are more frequent and severe in long bones compared with other bones.

In our study, spontaneous fractures of the femur were identified in both male and female *sfx*/*sfx* mice. Radiographs revealed numerous fractures of the femoral metaphysis where the diaphyseal shaft was dislocated and driven into the distal metaphysis in mice 6–7 weeks of age (Fig. 1). Fractures were also identified in the radiographs of smaller bones, such as the metacarpals (data not shown).

The mechanism behind the significantly reduced BMD was studied by measuring serum osteocalcin levels and performing dynamic histomorphometry. Serum osteocalcin levels were decreased by 70% in the *sfx*/*sfx* mice compared with the +/? mice (62.4 ± 32 versus 198 ± 64 ng/ml; $n = 8$, $p < 0.001$), suggesting a decrease in total osteoblast activity. Histomorphometry at the femoral mid-diaphysis revealed that bone area was decreased by 40% in the *sfx*/*sfx* mice compared with control mice (Table 2). To avoid fracture callus, histomorphometric analyses were carried out at the mid-diaphysis where there were no fractures. In addition, we killed mice at 5 weeks of age, before they developed fractures. Periosteal and endosteal perimeters were decreased by 13% and 11%, respectively, in the *sfx*/*sfx* mice compared with the +/? mice. Notably, the bone formation rate at the periosteum was strikingly compromised by >90% in the *sfx*/*sfx* mice, indicating a decrease in total osteoblastic activity. Furthermore, the periosteal mineral apposition rate was decreased by 80% in the *sfx*/*sfx* mice, implying an impaired differentiation and/or function of osteoblasts as the major cause for decreased bone formation. There was no detectable label at the endosteum of the *sfx*/*sfx* mice, implying that little or no bone formation occurs at the endosteum of the *sfx*/*sfx* mice. Accordingly, it was previously observed that the bones of *sfx* mice had reduced osteoid but normal osteoclasts.[6] Thus, based on the histomorphometric data, it can be concluded that an impairment of differentiated function of osteoblasts is the major cause for decreased bone formation in *sfx*/*sfx* mice.

Fine mapping and identification of the sfx candidate gene

In a previous study, it was shown that the *sfx* mutation is inherited as a recessive gene that maps to the middle of chromosome 14.[6] We mapped the region previously shown to contain the *sfx* locus more precisely by genotyping additional markers in this region. Table 3 shows the results of our haplotype analysis of 272 Balb/cBy-Cast F2 *sfx*/*sfx* mice for six markers near the *sfx* locus. No recombination between the *sfx* gene and D14Mit203 was detected in 272 *sfx*/*sfx* mice. In two mice, there were triple recombinations, with one recombination after D14Mit66 and two recombinations, one on each side of D14Mit203, which were confirmed by repeated genotyping. Based on these data, we concluded that the *sfx* gene was located near the D14Mit203 marker on chromosome 14, between 56.04 and 58.20 MB (NCBI database) or between 58.82 and 60.96 MB (Celera database). This 2-MB region contains ~30 genes based on the predicted genes in the Celera database (Table 4). There were several potential candidate genes, such as *Hox-related protein*, *exostosin-3 related*, *Frizzled 3,* and *Fbox only protein 16*, that were located within the 2-MB *sfx*

FIG. 1. X-ray of femur from control and *sfx* mice showing fracture. Radiograph of *sfx*/*sfx* mouse at 47 days showing the common characteristic telescoping impaction fracture of the femoral metaphysis, which has resulted in a severe shortening of the femur.

TABLE 2. DYNAMIC HISTOMORPHOMETRIC PARAMETERS AT THE FEMORAL MID-DIAPHYSIS OF 5-WEEK-OLD *sfx* AND CONTROL MICE

Parameter	*+/?*	*sfx/sfx*
Total area (mm^2)	1.434 ± 0.125	0.978 ± 0.108*
Bone area (mm^2)	0.705 ± 0.106	0.427 ± 0.111*
Medullary area (mm^2)	0.729 ± 0.046	0.551 ± 0.008*
Periosteal perimeter (mm)	4.443 ± 0.207	3.867 ± 0.100*
Periosteal BFR (10^{-3} mm/day)	14.951 ± 3.552	1.137 ± 0.692*
Periosteal BFR/bone surface	3.343 ± 0.657	0.296 ± 0.179*
Periosteal MAR (μm/day)	5.170 ± 1.782	1.128 ± 0.318*
Endosteal perimeter (mm)	3.139 ± 0.120	2.796 ± 0.113*
Endosteal BFR (10^{-3} mm/day)	5.015 ± 4.466	ND
Endosteal BFR/bone surface	1.548 ± 1.333	ND
Endosteal MAR (μm^{-1}/day)	2.507 ± 1.986	ND

All values are expressed as mean ± SD with an $n = 4$–5 per group.

BFR, bone formation rate; MAR, mineral apposition rate; ND, not detectable.

* $p < 0.01$ vs. control mice.

region. We initially sequenced the coding regions of these positional candidate genes and found no evidence for mutation in the coding region in them (Table 4).

We next performed a whole genome microarray analysis using 20,000 mouse oligonucleotide probes (Agilent) to identify genes differentially expressed in the bones of *sfx* and control mice. We reasoned that information on the molecular pathways affected in the bones of *sfx* mice would provide some knowledge on the potential candidate genes for *sfx*. Although several genes in the *sfx* locus were present in the microarray slide, we found none of these genes showed a significant change in expression in the bones of the *sfx* mice compared with control mice. Whole genome microarray analysis did, however, reveal that the expression of several genes related to mitochondrial energy metabolism was severely compromised in the bones of *sfx* mice compared with control mice (data not shown). Particularly, we found that the expression levels of a number of ATPases (Atpla3, Atp2c1, Atp5k, Atp5j, Atp5j2, Atp5g3, and Atp51) were significantly altered in the bones of *sfx* mice compared with control mice (data not shown).

To identify potential candidate genes in the *sfx* locus that could be involved in regulating energy metabolism, we searched for functional motifs in the 30 genes present near the *sfx* locus using the ScanProsite tool (Swiss Institute of Bioinformatics). This search led to the identification of two candidate genes, *mCG141014* (mCT 172717) and *mCG2517* (mCT 1325), which were located at 60.34 and 60.73 MB, respectively, in chromosome 14 (Celera database). The sequence analysis of the coding region of the *mCG141014* gene (similar to hypothetical protein XP_154842.1), which contains a ATP/GTP binding site (P-loop motif), revealed

Table 3. Haplotype Mapping of Markers in the *sfx* Candidate Region

	D14MIT66 *52.40*/55.18†*	*D14MIT88* *55.64/58.34*	*D14MIT235* *56.04/58.82*	*D14MIT203* *57.85/60.62*	*D14MIT123* *58.20/60.96*	*D14MIT143* *59.16/61.93*	*No. of mice*
	B	B	B	B	B	B	245
	H	B	B	B	B	B	6
	B	H	B	B	B	B	2
	H	H	B	B	B	B	2
	B	B	H	B	B	B	1
	H	H	H	B	B	B	3
	B	H	H	B	H	H	2
	B	B	B	B	B	H	11
Total recombination	11	9	6	0	2	13	

Two hundred seventy-two Balb/cBy-CAST F2 *sfx/sfx* mice were genotyped using six microsatellite markers for haplotype analysis. B represents Balbc/Balbc homozygous genotype for the indicated marker. H represents Balbc/CAST heterozygous genotype for the indicated marker.

No crossover occurred between the *sfx* gene and D14MIT203 marker in 272 Balb/cBy-CAST F2 *sfx/sfx* mice. Recombination between *sfx* gene and D14MIT235, and between *sfx* gene and D14MIT123, were detected in six and two mice, respectively. These data show that the *sfx* gene is located near the D14MIT203 marker.

* and † represent positions of markers in megabase according to NCBI database and Celera database, respectively.

Table 4. Sequencing Results of Genes Located in the *sfx* Candidate Region

mCT	*Location (MB)*	*Gene name*	*Coding region sequenced; results*
54441	59.35	Unknown, similar to hypothetical protein	480-930 bp; No mismatch
1541	59.41	Kinesin 13A2	75-5910 bp; No mismatch
1547/182002	59.58	Riken cDNA, Hox related protein	332-1547 bp; No mismatch
1546	59.72	cDNA, similar to hypothetical protein	4-1826 bp; No mismatch
171624	59.81	Extl3, exostosin-3 related	332-1547 bp; No mismatch
155294	59.93	Unknown	313-2300 bp; No mismatch
1543	59.96	Frizzled 3	121-1125 bp; No mismatch
173406	60.02	Fbox only protein 16	130-1210 bp; No mismatch
155292	60.09	Unknown pseudo	ND
1542	60.13	Papillomavirus regulatory factor, zinc finger protein	31-1585 bp; No mismatch
1545	60.15	Nociceptin, opiod receptor	ND
1321/180144	60.28	RNA polymerase II associated histone acetyl transfer	84-1724 bp; No mismatch
172717	60.34	Similar to hypothetical protein, NLS BP	303-2704 bp; No mismatch
1335	60.41	Macrophage scavenger receptor type I and type II	ND
172306	60.55	Protein serine/threonine kinase receptor related	281-1467 bp; No mismatch
180147	60.59	Riken cDNA, hypothetical protein	91-1874 bp; No mismatch
1337	60.59	Similar to hypothetical protein, no domain hits	106-730 bp; No mismatch
1342	60.67	Macrophage scavenger receptor like	ND
126977	60.71	Protein phosphatase pp2A, pseudo exon	ND
1325	60.73	Gluconolactone oxidase, vitamin metabolism	Gene deletion
1330	60.77	ADAM 2, MMP	ND
126972	60.79	Translocase of inner mitochondrial membrane	22-993 bp; No mismatch
1333	60.83	Epoxide hydrolase, isoprenoid catabolism	ND
1327	60.91	Neuronal acetylcholine receptor protein alpha2 chain	ND
1322/128189	60.9	PTK2 protein tyrosine kinase beta	ND

This gene list was prepared according to Celera database. mCT numbers represent transcript numbers for various genes provided in the Celera database. The location of genes in chromosome 14 is based on information provided by the Celera database. No product could be amplified for mCT 155292, mCT 126977, mCT 1333, and mCT 1327 using cDNA prepared using RNA from bone.

ND, not determined.

no sequence polymorphisms between the *sfx* and control mice (Table 4). We next focused on the second candidate gene, *mCG2517*, which encoded a hypothetical protein (BC019856) similar to GULO, an enzyme involved in the synthesis of ascorbic acid. Because the expression levels of several dehydrogenases were altered in the *sfx* mice and because *mCG2517* contained a FAD binding site, we considered this gene a strong candidate for *sfx*. To sequence the coding region of *mCG2517*, we amplified the coding region using exon-specific primers and cDNA prepared from bones of control and *sfx* mice as templates (Table 5). To our surprise, we were able to amplify PCR products for cDNA from the control mice, but not the *sfx* mice, using a number of primers in the coding region of *GULO* (Fig. 2A). The six primer sets used for evaluation of *GULO* expression covered the entire coding region of the *GULO*

TABLE 5. PRIMERS USED FOR PCR AND CORRESPONDING REGIONS OF GULO cDNA AMPLIFIED IN CHROMOSOME 14

Primer name	*Sequence*	*Amplified region (bp)*	*Size of PCR product (bp)*	*PCR product*	
				+/?	*sfx/sfx*
GULO coding-1 forward	GTTGCCTGACCACTGCATCT	12–448	437	+	–
GULO coding-1 reverse	ACGGCTCCCAGATTAGACAG				
GULO coding-2 forward	CAGATGGGCAAGATGAACC	311–701	391	+	–
GULO coding-2 reverse	GAAGGAAAGGATGTCTCCA				
GULO coding-3 forward	CTGCCTGGGTGTTATCCTCA	326–993	368	+	–
GULO coding-3 reverse	TCTTGTGGCTGAGGTTGCTG				
GULO coding-4 forward	GGCTGGATCAACCGCTTCTT	921–1325	345	+	–
GULO coding-4 reverse	TTCCTGGTGCAATTGTGGG				
GULO coding-5 forward	TATGTACAGGCCCTATGGGA	1205–1542	338	+	–
GULO coding-5 reverse	TTGTGTTCAGGAGAGGTCGT				
GULO coding-6 forward	GTAGAAGCAGAAGCAAGCTG	1435–1821	387	+	–
GULO coding-6 reverse	ATGCTACCTCTGTTGCCAAG				

Primers were designed along the entire coding region of GULO (BC019856.1). The corresponding regions of mRNA sequence amplified by different overlapping primer sets were identified by Contig Express (Vector NTI, InfoMax, Bethesda, MD, USA). All six primer sets failed to produce PCR products using cDNA prepared from bones of *sfx/sfx* mice. However, PCR products of anticipated size could be produced using cDNA from the bones of +/? mice as a template. cDNA prepared from four to six *sfx/sfx* and corresponding control mice were used as templates for PCR amplification. The results were confirmed in at least one duplicate experiment.

These data show that GULO transcript is absent in *sfx/sfx* mice.

+, PCR product of right size was amplified; –, no PCR product could be amplified.

sequence (BC019856.1) as shown in Table 5. The *GULO* coding 1 forward primer matched to 57,994,786 to 57,994,767-bp region in mouse chromosome 14, whereas the *GULO* coding six reverse primers matched to the 57,972,836 to 57,972,817-bp region (http://genome.ucsc.edu). We therefore studied the possibility that the *sfx* phenotype is caused by a deletion of the *GULO* gene.

Mapping of GULO deletion in sfx mice

To confirm and examine the extent of chromosomal deletion in our *sfx* mice, we used DNA isolated from *sfx*/*sfx* and +/? control mice to amplify the 5′ end, intronic, and 3′ end of *GULO* using appropriate primers throughout the *GULO* gene (Table 6). The transcribed region of the *GULO* gene resides in chromosome 14 between 57,994,797 and 57,972,426 bp (encodes mRNA BC019856.1; http://genome.ucsc.edu). Consistent with the data using cDNA from bones, PCR amplification of genomic DNA from *sfx* mice failed to generate PCR products for primers located within the transcribed region of the *GULO* gene (Table 6; Fig. 2B). These data provide evidence that the transcribed region of the *GULO* gene is deleted in the *sfx* mice. To identify the extent of chromosome 14 deletion, we designed additional primers at both 5′ and 3′ ends of the *GULO* gene and generated PCR products using DNA from control and *sfx* mice (Table 6; Fig. 2B). Our first sets of primers were ~3000 bp apart at both the 5′ and 3′ ends of the transcribed region of the *GULO* gene. Subsequently, we refined the deletion more precisely by designing additional primers in the region of interest. Using this strategy, we determined that the deletion occurs after 58,008,985 bp and before 57,970,574 bp at the 5′ and 3′ ends of the transcribed region of the *GULO* gene, respectively (Table 6; Fig. 2B). To determine if the chromosomal deletion in *sfx* mice extended to the neighboring genes, we designed a number of PCR primers for the transcribed region of genes, *Adam 2* and *C130058N24Rik*, that were located upstream or downstream, respectively, of the *GULO* gene in chromosome 14. We were able to amplify PCR products of anticipated size using DNA from both *sfx* and control mice for both of these genes (data not shown), indicating that the deletion was confined to the *GULO* gene in *sfx* mice.

To identify the exact location of deletions in chromosome 14 in the *sfx* mice, we generated PCR products using GULO 5′-2A forward primer and 3′-1A reverse primer (Table 6). Figure 2C shows the results of PCR amplification of DNA from +/+, +/*sfx,* and *sfx*/*sfx* mice. A PCR product of ~700 bp was amplified using DNA from *sfx*/+ and *sfx*/*sfx* mice but not +/+ mice (product was too large to amplify because there was no deletion). We sequenced the amplified product to identify the exact location of deletion. BLAT search of mouse genome (http://genome.ucsc.edu) using nucleotide sequence of PCR product from *sfx* mice revealed 100% alignment with 58,009,113 to 58,008,747 bp and with 57,970,600 to 57,970,381 bp of mouse genome sequence in chromosome 14. Based on the sequence information and the PCR data, we determined that a 38,146-bp region encompassing 58,008,746 to 57,970,601 bp of chromosome 14 containing the entire transcribed region of the *GULO* gene is deleted in *sfx* mice (Fig. 2D). Because the deleted region in chromosome 14 does not contain any other predicted genes and because there was no polymorphism in the coding region of other potential candidate genes in the *sfx* locus (Table 4), we concluded that *GULO* is the *sfx* gene.

To further confirm the deletion of *GULO* in *sfx* mice, we performed PCR amplification of *GULO* using DNA from several inbred strains of mice and found that *GULO* is only absent in *sfx* mice and present in all other stains of mice we tested (data not shown). Surprisingly, Agilent microarray data revealed no difference in expression levels of *GULO*

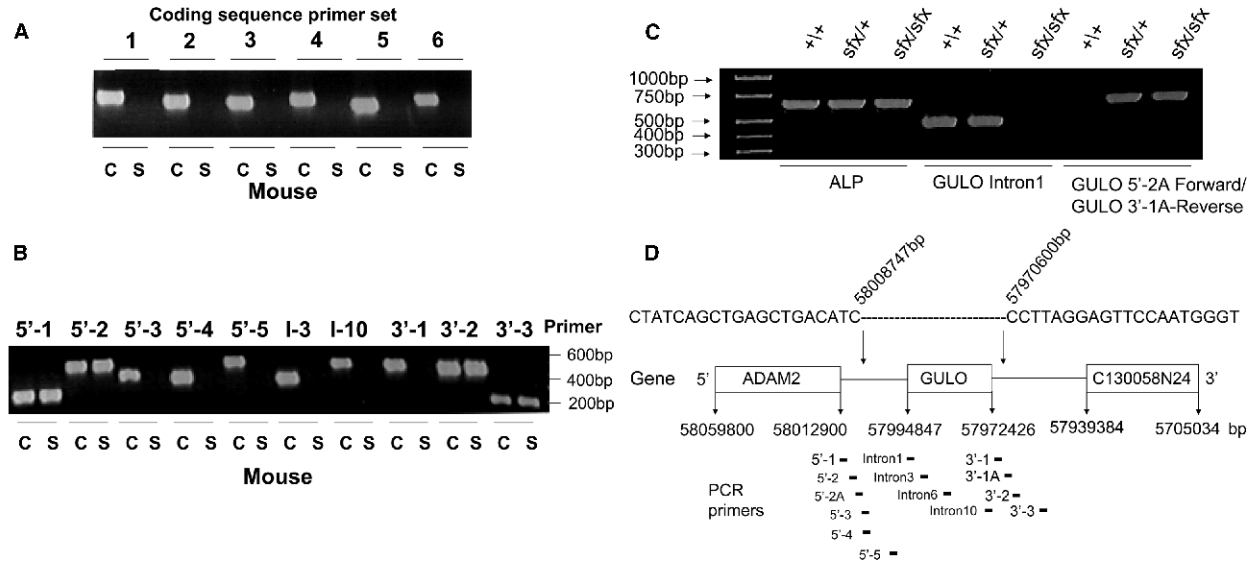

FIG. 2. (A) PCR amplification of GULO coding region using cDNA from bones of control and *sfx* mice; 200 ng of RNA isolated from bones of +/? and *sfx*/*sfx* mice was used for preparation of cDNA. An aliquot of cDNA was used for PCR amplification using primers that cover the entire coding region of *GULO* (Table 5). PCR products of anticipated size were amplified for cDNA from control mice but not for cDNA from *sfx* mice. C, control mice; S, *sfx*/*sfx* mice. (B) PCR amplification of DNA using various primers; 20 ng of DNA isolated from spleen of +/? and *sfx*/*sfx* mice was used for PCR amplification using various sets of primers in the 5′UTR, intronic, and 3′UTR regions of *GULO*. The sequence of primers used and the region of chromosome 14 amplified by the various primers are shown in Table 6. PCR products of only selected primers are shown for the sake of space. No PCR product was seen for chromosomal region encompassing 58,008,858–57,971,069 bp using DNA from *sfx*/*sfx* mice. (C) PCR amplification of DNA using *sfx*/*sfx*, *sfx*/+, and +/+ mice with chromosome 14 forward primer (58,009,161–58,009,182 bp) and reverse primer (57,970,352–57,970,371 bp). Wildtype (+/+), heterozygous (*sfx*/+), and *sfx* (*sfx*/*sfx*) mice were identified by genotyping using two sets of primers. *ALP* gene was used as an internal control. *GULO* intron1 primer set in the transcribed region of *GULO*-amplified PCR product of anticipated size for DNA from both wildtype and heterozygous mice but not for *sfx* mice. Forward primer for *GULO* 5′-2A and reverse primer for *GULO* 3′1A, which are located at the 5′ and 3′ ends of chromosome 14, deletion in *sfx* mice amplified PCR product of ~700 bp for both *sfx* homozygous and heterozygous mice but not for wildtype mice. Heterozygous mice have one copy of intact and one copy of deleted chromosome 14 and are therefore positive for both sets of primers. *sfx* homozygous mice have both copies of deleted chromosomes and are therefore negative for *GULO* intron 1 primer set but positive for *GULO* 5′-2A forward/*GULO* 3′-1A reverse primer set. Wildtype mice have both copies of intact chromosome 14 and are therefore positive for *GULO* intron 1 primer set and negative for *GULO* 5′-2A forward/*GULO* 3′-1A reverse primer set, because the product is too large to amplify. The PCR product from *sfx*/*sfx* homozygous mice was used for sequencing. (D) Map of deletion in chromosome 14 in *sfx* mice. The sequence of PCR product amplified using *GULO* 5′-2A forward and *GULO* 3′-1A reverse primer set was BLAT searched to identify matching a sequence in mouse chromosome 14. The nucleotide sequence of PCR product revealed a 100% sequence identity with a 58,009,113–58,008,747-bp segment and a 57,970,600–57,970,381-bp segment of mouse chromosome 14. Based on these data, we have mapped the deletion to a region between 58,008,747 and 57,970,600 bp (38,146 bp) in chromosome 14 reverse strand. Box labeled GULO represents the transcribed region of *GULO*. The position of the PCR primers included in Table 6 are shown here as thick black lines.

between the bones of the control and *sfx* mice. The 60-mer oligo probe used in the Agilent microarray falls within the deleted region of chromosome 14 in sfx mice (57,973,026-57,972,967 bp). Accordingly, our *GULO* coding primer set that amplified a region from 57,973,204 to 57,972,817 bp was positive for cDNA from control mice and negative for cDNA for *sfx* mice. To determine whether the *GULO* oligo probe used in the Agilent microarray cross-hybridized with one or more transcripts expressed in bone and contributed to the apparent discrepancy, we performed a NCBI BLAST search (http://www.ncbi.nim.nih.gov/BLAST) and found no significant cross-reactivity with other mouse transcripts besides *GULO*. It is therefore unclear why the *sfx* mice have measurable mRNA for the *GULO* gene by Agilent microarray.

Ascorbic acid deficiency in sfx mice

If our prediction that the entire transcribed region of the *GULO* gene is deleted in chromosome 14 is correct, *sfx* mice should be deficient in ascorbic acid. Therefore, we measured serum ascorbic acid levels in *sfx* and corresponding control mice. Figure 3 shows there was no detectable level of ascorbic acid in the *sfx*/*sfx* mice, whereas control mice showed the expected levels of ascorbic acid in their blood. The lack of ascorbic acid in the serum of 6-week-old *sfx* mice is not surprising because the diet we used contained no vitamin C.

Reversal of sfx phenotype by treatment of sfx/sfx mice with ascorbic acid

If deletion of *GULO* is responsible for the *sfx* phenotype, it follows that we should be able to correct the phenotype by giving ascorbic acid to *sfx*/*sfx* mice. To obtain further proof that *GULO* is the *sfx* gene, we treated *sfx*/*sfx* mice with ascorbic acid in their drinking water (330 mg/liter). Figure 4 shows that treatment of *sfx*/*sfx* mice at weaning with ascorbic acid for 3 weeks led to a reversal of the *sfx*

TABLE 6. PRIMERS USED FOR PCR AND CORRESPONDING REGIONS OF GENOMIC SEQUENCE AMPLIFIED IN CHROMOSOME 14

Primer name	*Sequence*	*Amplified region (bp)*	*Size of PCR product (bp)*	*PCR product*	
				+/?	*sfx/sfx*
GULO 5′-1 forward	5′AAATATGCGAACTGGGCAGTGG3′	58,011,719–58,011,452	267	+	+
GULO 5′-1 reverse	5′CAACATGTGCATGTGTGCCTGA3′				
GULO 5′-2 forward	5′CTCTCTTTCCAGTGATGGCTGA3′	58,009,914–58,009,420	494	+	+
GULO 5′-2 reverse	5′TGCTATCAGTCAGTGTTCGCTG3′				
GULO 5′-2A forward	5′TGACCTTAGAGGAGAGATGC3′	58,009,182–58,008,985	198	+	+
GULO 5′-2B reverse	5′TGAGTGTCCAACACAGTCTG3′				
GULO 5′-3 forward	5′CTGCCCACTATCCTATCACTGA3′	58,008,858–58,008,474	384	+	–
GULO 5′-3 reverse	5′CTCTTTCCCTTCCTCACTCTGT3′				
GULO 5′-4 forward	5′GGCTACAAAGTTGCTTCATCGG3′	58,008,578–58,008,196	382	+	–
GULO 5′-4 reverse	5′AGCACATTAGAACATGCCACCC3′				
GULO 5′-5 forward	5′GGCATCTATGGTGACTGGAAGA3′	57,998,175–57,997,655	520	+	–
GULO 5′-5 reverse	5′CGGTAACTCACAGAAATCGTCC3′				
GULO intron1 forward	5′GTTGCCTGACCACTGCATCT3′	57,994,786–57,994,324	552	+	–
GULO intron1 reverse	5′AGCCAGATACGGTGGCTCTT3′				
GULO intron3 forward	5′AGCCAACCAGCAGTACCTAAGT3′	57,990,865–57,990,515	350	+	–
GULO intron3 reverse	5′TAAGGGCTGAGAAGGAAGAGAC3′				
GULO intron6 forward	5′CCACATTTCCACCAGAGTACCA3′	57,984,589–57,984,069	520	+	–
GULO intron6 reverse	5′CCCTTGCTTGCTTACACTTTGG3′				
GULO intron10 forward	5′CAGTGCAGCCTTGCTTGACATA3′	57,973,399–57,972,916	483	+	–
GULO intron10 reverse	5′GACCAAATCCTTAGCCTGGACA3′				
GULO 3′-1 forward	5′GCTCTTCAACCAAAGGTAGG3′	57,971,524–57,971,069	455	+	–
GULO 3′-1 reverse	5′GGACAGAAGGACATTTGAGG3′				
GULO 3′-1A forward	5′CATTCTCTCTCTGAGCTGGT3′	57,970,574–57,970,352	223	+	+
GULO 3′-1A reverse	5′TGGGACAGAACTAACAGGAG3′				
GULO 3′-2 forward	5′CGAGTTAACAGATGGATGCCAG3′	57,970,139–57,969,718	421	+	+
GULO 3′-2 reverse	5′CCTCTCTCAAACATCTCCACCA3′				
GULO 3′-3 forward	5′CCCTGTGGCTGAGGATATTC3′	57,962,402–57,962,217	188	+	+
GULO 3′-3 reverse	5′ACACACTTGTGCTCTCTGGG3′				

Different primer sets were used to amplify various regions of the *GULO* gene. The corresponding regions of genomic sequence amplified in chromosome 14 were identified by BLAT search of mouse genome sequence (http://genome.ucsc.edu). The DNA from four to six *sfx/sfx* and corresponding control mice were used for evaluation. The results were confirmed in at least one independent experiment. Only informative primers tested are listed for the sake of space.

These data show that the region between 58,008,858 and 57,971,069 bp could not be amplified using DNA from *sfx* mice.

+, PCR product of right size was amplified; –, no PCR product could be amplified.

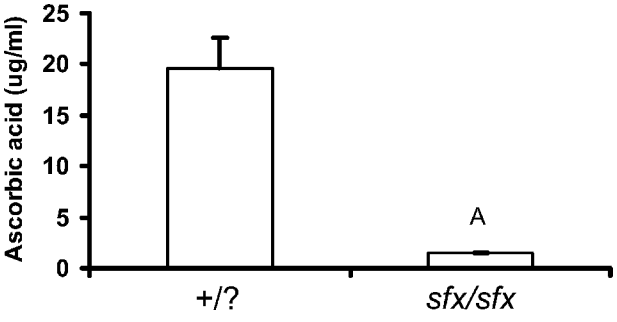

FIG. 3. Serum levels of ascorbic acid in *sfx/sfx* and corresponding *sfx/?* control mice. Serum from 6-week-old *sfx/sfx* and corresponding control mice were used for measurement of ascorbic acid by a commercial kit. Values are mean ± SD of five mice per group. $^{A}p < 0.001$ vs. control mice. Ascorbic acid levels were undetectable in *sfx/sfx* mice.

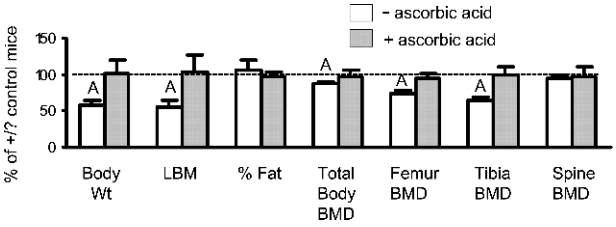

FIG. 4. Effects of ascorbic acid treatment on the musculoskeletal parameters in *sfx* mice. *Sfx/sfx* and +/? mice were given ascorbic acid in the drinking water (330 μg/ml), and the water was changed every other day. Control mice were given drinking water without ascorbic acid. Ascorbic acid treatment began at 3 weeks of age, the animals were killed at 6 weeks of age, and musculoskeletal parameters were measured by PIXImus. Control and *sfx/sfx* mice receiving drinking water were killed at 5 weeks of age because fractures start to occur at 5 weeks in *sfx/sfx*. Values are percent corresponding control (+/?) mice treated with or without ascorbic acid and are mean ± SD of eight mice per group. Ascorbic acid treatment fully corrected the *sfx* phenotype. $^{A}p < 0.01$ vs. *sfx/?* mice.

phenotype to near normal levels for both the body weight and musculoskeletal parameters that we studied. The homozygous *sfx/sfx* mice treated with ascorbic acid grew normally during puberty and acquired bone mass comparable with that of corresponding control mice fed with a similar amount of ascorbic acid. Whereas treatment of *sfx* mice with ascorbic acid corrected the musculoskeletal deficits,

Table 7. Expression Levels of *GULO* in Various Tissues

Tissue	*GULO (Ct)*	*PPIA (Ct)*	*ΔCt*
Liver	25.8 ± 0.75	18.6 ± 0.2	7.2 ± 0.6
Kidney	34.7 ± 1.1	17.5 ± 1.2	17.2 ± 1.2
Bone	36.1 ± 0.9	17.2 ± 0.5	18.9 ± 1.0
Brain	35.0 ± 0.8	16.2 ± 0.3	18.8 ± 0.6
Muscle	34.6 ± 2.2	18.5 ± 0.9	16.1 ± 1.8
Thymus	34.2 ± 1.0	15.5 ± 0.6	18.7 ± 0.4
Spleen	34.8 ± 0.5	16.7 ± 0.5	18.1 ± 0.4
Adrenal gland	29.2 ± 1.4	17.4 ± 0.8	11.8 ± 2.1

RNA extracted from three to six mice for various tissues were used for *GULO* expression by real-time PCR. Ct (cycle threshold) values represent the cycles at which samples reach a fluorescent intensity above background. ΔCt values were calculated by subtracting the Ct values for the housekeeping gene (*PPIA*) from the *GULO* gene. Values are mean ± SD of three to six independent RNA sample for various tissues. The expression of *GULO* is highest in liver compared with other tissues.

ascorbic acid treatment of control mice for 3 weeks had no significant effect on body weight (19.4 ± 0.6 versus 18.9 ± 1.2 g), lean body mass (15.4 ± 0.8 versus 14.7 ± 1.3 g), total body BMD (40.4 ± 2.3 versus 42.0 ± 2.1 mg/cm^2), or femur BMD (59.7 ± 3.2 versus 62.0 ± 5.0 mg/cm^2), suggesting that the endogenously produced vitamin C was adequate for normal growth in the control mice. Furthermore, the *sfx*/*sfx* mice fed with ascorbic acid in their drinking water were fertile, showed no evidence of fractures, and produced normal sized litters (8.9 ± 2.1 versus 9.8 ± 1.7 offspring/litter, $n = 10$ litters). We currently have several of the *sfx/sfx* mice fed with ascorbic acid that are >6 months old and exhibit no signs of scurvy or other features of *sfx* phenotype. These data provide convincing evidence that a deficiency in ascorbic acid caused by a disruption of the *GULO* gene contributes to the observed phenotype in the *sfx* mice.

GULO is expressed in a number of tissues

To examine if GULO is involved in regulating local production of ascorbic acid in various cell types, we evaluated expression levels of GULO in various tissues by real-time PCR. Accordingly, we found evidence for expression of *GULO* in a number of tissues, including liver, adrenal gland, muscle, bone, kidney, brain, thymus, and spleen (Table 7). The magnitude of *GULO* expression is >20-fold higher in the liver than in a number of other tissues, suggesting that the liver is the major endocrine source of ascorbic acid in blood. Because the magnitude of GULO expression in various tissues did not seem to correlate with the severity of phenotype, the extent to which the local production of ascorbic acid contributes to regulating the differentiated functions of cell types in various tissues remains to be determined.

Impaired osteoblast differentiation in sfx phenotype is corrected by ascorbic acid treatment

We next sought to determine if the deficiency in bone formation in *sfx*/*sfx* mice is caused by impairment in the formation of mature osteoblasts. To this end, we cultured bone marrow stromal cells from *sfx*/*sfx* and +/? mice and examined the ability of these cells to form mineralized nodules in vitro. Figure 5A shows that bone marrow stromal cells from *sfx*/*sfx* mice produced very few or no mineralized nodules when grown in mineralization medium containing 50 μg/ml ascorbic acid. However, treatment of bone marrow stromal cells from *sfx*/*sfx* mice with 300 μg/ml ascorbic acid 2-phosphate, a long acting vitamin C derivative,[21] led to a reversal of mineralization defects. The percentage of mineralized nodule area was 0.29 ± 0.2% and 10.5 ± 4.8% (SD; $n = 3$, $p < 0.05$), respectively, in bone marrow cultures derived from *sfx* and wildtype mice cultured in mineralization media. Addition of 300 μg/ml ascorbic acid 2-phosphate to bone marrow cells derived from *sfx* mice increased the mineralized area by 30-fold (8.9 ± 4.2%, $p < 0.05$ versus mineralization media). Furthermore, we found that ascorbic acid treatment of bone marrow stromal cells from *sfx* mice for 12 days increased expression levels of type I collagen, alkaline phosphatase (ALP), and osteocalcin by 6-, 8-, and 20-fold, respectively, ($p < 0.001$) compared with cells cultured without ascorbic acid (Fig. 5B). Figure 5C shows that osteocalcin levels were undetectable in the conditioned medium of bone marrow stromal cells derived from *sfx/sfx* mice cultured for 24 days in DMEM that contained no ascorbic acid. Treatment of bone marrow stromal cells from *sfx* mice with 300 μg/ml ascorbic acid 2-phosphate increased osteocalcin levels by >50-fold at day 24. These and other in vitro data[21–23] provide convincing evidence that ascorbic acid is an important regulator of differentiated functions of osteoblasts.

DISCUSSION

We have provided several very strong lines of evidence that the *GULO* gene is the *sfx* gene. The importance of the *sfx* gene in skeletal biology is underscored by the fact that only a select few genetic abnormalities lead to spontaneous fracture at a young age. If the *sfx* phenotype is caused exclusively by a deficiency in vitamin C resulting from a deletion of the *GULO* gene, it stands that the *sfx* phenotype should be completely reversed by supplemental administration of vitamin C, as was found in our study. Furthermore, the in vitro phenotype (i.e., impairment in the differentiation of bone marrow stromal cells into osteoblasts) was as dramatic as the fracture phenotype in vivo and was also rescued by vitamin C treatment.

In addition to creating these dramatic skeletal phenotypes, vitamin C deficiency also causes widespread abnormalities in multiple organs. In this regard, the epidemiology of scurvy or vitamin C deficiency has differed from the past to present. During the 15th and 17th centuries, scurvy emerged as a problem for maritime explorers when it was a fatal disease among sailors. The symptoms and signs of patients with vitamin C deficiency included inability to walk, tenderness in lower limbs, subperiosteal bleeding, gum hypertrophy and bleeding, and anemia.[7–10] The most common cutaneous findings are follicular hyperkeratosis, perifollicular hemorrhages, ecchymoses, xerosis, leg edema, poor wound healing, and bent or coiled body hairs.[7] Although scurvy is currently uncommon because of food fortification with vitamin C, the disease occasionally occurs in some parts of the world among refugees and children fed

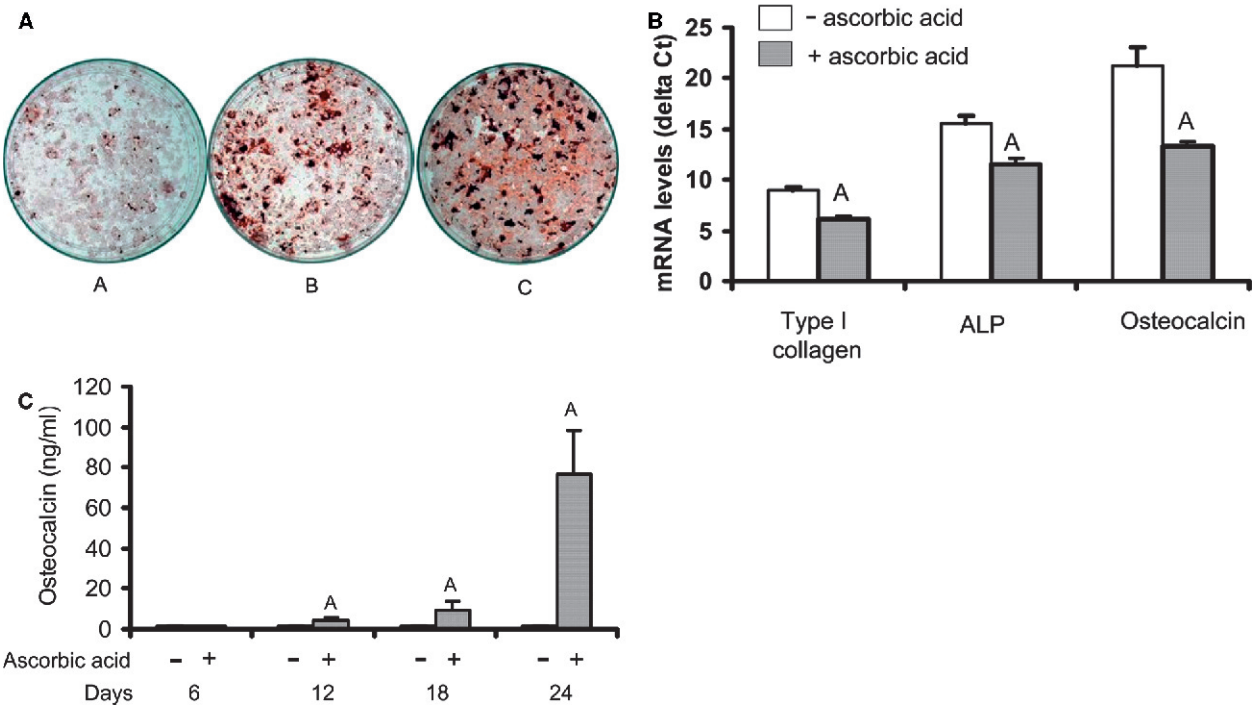

FIG. 5. (A) Effects of ascorbic acid treatment on formation of mineralized nodules in bone marrow stromal cells derived from *sfx* and control mice. Bone marrow stromal cells from *sfx*/*sfx* mice were cultured with mineralization protocol for 30 days (A) without and (B) with long acting ascorbic acid 2-phosphate (300 μg/ml) and mineralized nodule visualized by alizarin red staining. Bone marrow stromal cells from wildtype mice were cultured in mineralization protocol in C. Bone marrow stromal cells from *sfx*/*sfx* mice formed very few mineralized nodules compared with stromal cells from +/? mice, which was rescued by ascorbic acid 2-phosphate. Three replicate cultures per group were performed, and the results were confirmed in an independent experiment. (B) Effects of ascorbic acid treatment on expression levels of type 1 collagen, ALP, and osteocalcin in bone marrow stromal cells derived from *sfx/sfx* mice. Bone marrow stromal cells from *sfx/sfx* mice were cultured in DMEM containing 10% calf serum and β-glycophosphate 12 days with or without ascorbic acid. RNA was extracted and used for real-time PCR analysis using specific primers. ΔCt values were determined by subtracting Ct values for reference gene (PPIA) from Ct values for test genes. Values are mean ± SD of six replicate cultures. $^{A}p < 0.001$ vs. vehicle-treated control cultures. The lower ΔCt values in the ascorbic acid treated cultures represent increased expression of type 1 collagen, ALP, and osteocalcin compared with vehicle-treated control cultures. (C) Effects of ascorbic acid treatment on osteocalcin levels in conditioned medium of bone marrow cells derived from *sfx/sfx* mice. Cells were cultured in DMEM containing 10% calf serum as described for B and treated with vehicle or 300 μg/ml ascorbic acid 2-phosphate. At days 6, 12, 18, and 24, conditioned medium was collected and used for osteocalcin measurements. Values are mean ± SD of six replicate cultures. Osteocalcin levels were below detection limit (<1.56 μg/ml) in vehicle-treated bone marrow cells. $p < 0.001$ in ascorbic acid treated cultures vs. control.

improperly by their parents.[7–10] We found that s*fx* mice exhibited several features common to scurvy. For example, *sfx* mice exhibit significantly reduced body size, thymus, and spleen weights, as well as lower red and white blood cell counts, compared with age-matched control mice.[6] Based on our observations that *sfx* mice exhibit symptoms of scurvy syndrome, as well as documented observations in other studies,[24,25] we maintain that vitamin C deficiency can affect nearly every organ in the body. With regard to future studies, the bone phenotype is readily quantifiable and serves as an effective model for evaluating the effects of vitamin C deficiency on the body. In addition, if other cell types behave similarly to bone cells, then one would expect a generalized impairment in cell differentiation in response to ascorbic acid deficiency, which can be readily studied using osteoblasts in vitro.

The terminal step in the biosynthesis of l-ascorbic acid in mammals is dependent on GULO (EC 1.1.3.8), which is present in several mammalian species, including mice, rats, and pigs, but not in humans.[26] In previous studies, it was found that a particular strain of rat, the osteogenic disorder rat (ODS rat), developed signs characteristic of a vitamin C–deficient animal, including bleeding tendencies, skeletal abnormalities, and reduced GULO activity.[27,28] In the ODS rat, an A-G transition leads to a 61Cys-61Tyr substitution, which is responsible for the dramatic reduction in GULO enzyme activity.[29] More recently, Maeda et al.[30] generated a vitamin C–deficient ($GULO^{-/-}$) mouse strain by deleting exons III and IV through homologous recombination and found aortic wall damage in mice lacking functional GULO. In these studies, it was observed that the body weights of homozygous pups born to heterozygous mothers showed no variation at 21 days of age from their littermate controls. However, after weaning onto regular chow containing 110 mg/kg of ascorbic acid, the homozygotes showed very little growth, and after 40 days of age, they began to lose weight. We believe that the phenotype is more severe in the *sfx* mice because the laboratory chow used in our study contained no vitamin C.

Our data that heterozygous mice grow normally suggest

that a single copy of *GULO* is sufficient to produce adequate levels of ascorbic acid for normal growth in mice. The reason why the *sfx*/*sfx* mice grow normally until they are weaned is likely because of the presence of ascorbic acid in high concentrations in the mothers' milk.[13] On weaning, the *sfx*/*sfx* mice are completely deprived of ascorbic acid because the laboratory chow used in this study does not contain ascorbic acid. The lack of ascorbic acid during the pubertal rapid growth phase leads to little or no new bone formation, and as a consequence, fractures occur.

Although the observation that ascorbate deficiency led to diminished ALP in mineralized tissues was first published over 50 years ago,[31] the molecular pathways by which ascorbic acid deficiency leads to impaired bone formation are still poorly understood. In this regard, the most well-documented effect of ascorbate is on hydroxylation of prolyl and lysyl residues, which are necessary for the formation of stable triple helical collagen.[32] Several laboratories have shown that treatment of osteoblasts with ascorbic acid increased expression of specific genes associated with the osteoblast phenotype, including type I collagen, ALP, and osteocalcin.[22,33–35] With regard to the question of how ascorbic acid promotes transcriptional activity of genes, Xiao et al.[36] have shown that ascorbic acid treatment stimulates promoter activity of the *osteocalcin* gene by up-regulating the binding of osteoblast-specific factor 2 to an osteoblast-specific element in the promoter region. Thus, one way ascorbic acid treatment may promote differentiation is by activating the transcription of key genes involved in producing extracellular matrix proteins. A number of alternate mechanisms have been proposed to explain the mechanism by which ascorbic acid stimulates expression of bone formation marker genes, which include ascorbic acid–induced alterations in extracellular matrix and changes in the availability of IGF-I, extracellular calcium, or ATP.[37–39]

It is well established that ascorbic acid is necessary for the in vitro differentiation of osteoblasts.[22,33–35,40–42] The ability of ascorbic acid to promote differentiation is not specific to osteoblasts, because studies have shown that ascorbic acid also induces differentiation in a variety of cell types including myoblasts, adipocytes, and chondrocytes.[43–45] More recently, ascorbic acid has been shown to enhance differentiation of embryonic stem cells into cardiac myocytes.[46] Furthermore, Yu et al.[47] have recently shown that treatment of mesencephalic precursor cells with ascorbic acid increases their differentiation into dopaminergic neurons. Consistent with these in vitro data, our findings provide the first genetic evidence for an important role for ascorbic acid in regulating differentiated functions of osteoblasts in vivo. Our future studies will address the molecular mechanisms by which ascorbic acid deficiency regulates differentiated cell function using osteoblasts derived from *sfx* mice as our model.

Surprisingly, bone accretion is compromised much more in the long bones of *sfx* mice compared with vertebrae. Accordingly, the magnitude of total body BMD (excluding calvaria) deficit is less compared with femur or tibia BMD deficit in the *sfx* mice. At present, we have no experimental data to provide an explanation for the differential effects of ascorbic acid deficiency in the long bones versus vertebrae.

Although these findings are based on studies using a mouse model, we believe that the findings of this study have strong clinical implications. It is well known that humans depend on their diet for vitamin C because they lack the *GULO* gene and therefore cannot synthesize vitamin C. Based on our data that *sfx* mice with a complete deficiency in vitamin C form very little new bone, we believe that adequate vitamin C intake during the early active growth period may be critical in attaining an optimal peak BMD in humans as well. Furthermore, these findings also indicate that vitamin C deficiency may play a critical role in some of the skeletal abnormalities observed in the elderly, a segment of the population particularly susceptible to malnourishment. In fact, clinical epidemiological studies support this view.[48–50] Finally, in light of these findings, it is possible that a subclinical vitamin C deficiency impairs skeletal development during puberty. Further studies are needed to evaluate the extent to which vitamin C deficiency may contribute to the development of peak BMD during puberty and to the decline in osseous tissue during aging.

ACKNOWLEDGMENTS

We thank Chandrasekar Kesavan and Alice Kramer for technical assistance and Sean Belcher and Shelley Levtzow for administrative assistance. This study was supported by funds from NIH (AG19698). All work was performed at facilities provided by the Jerry L. Pettis Memorial VA Medical Center in Loma Linda, CA.

REFERENCES

1. Greendale GA, Barrett-Connor E, Ingles S, Haile R 1995 Late physical and functional effects of osteoporotic fracture in women: The Rancho Bernardo Study. J Am Geriatr Soc **43:**955–961.
2. Ray NF, Chan JK, Thamer M, Melton LJ III 1997 Medical expenditures for the treatment of osteoporotic fractures in the United States in 1995: Report from the National Osteoporosis Foundation. J Bone Miner Res **12:**24–35.
3. Melton LJ III 2003 Adverse outcomes of osteoporotic fractures in the general population. J Bone Miner Res **18:**1139–1141.
4. Baylink DJ, Strong DD, Mohan S 1999 The diagnosis and treatment of osteoporosis: Future prospects. Mol Med Today **5:**133–140.
5. Baldock PA, Eisman JA 2004 Genetic determinants of bone mass. Curr Opin Rheumatol **16:**450–456.
6. Beamer WG, Rosen CJ, Bronson RT, Gu W, Donahue LR, Baylink DJ, Richardson CC, Crawford GC, Barker JE 2000 Spontaneous fracture (sfx): A mouse genetic model of defective peripubertal bone formation. Bone **27:**619–626.
7. Hirschmann JV, Raugi GJ 1999 Adult scurvy. J Am Acad Dermatol **41**;:895–906.
8. Oeffinger KC 1993 Scurvy: More than historical relevance. Am Fam Physician **48:**609–613.
9. Ratanachu-Ek S, Sukswai P, Jeerathanyasakun Y, Wongtapradit L 2003 Scurvy in pediatric patients: A review of 28 cases. J Med Assoc Thai **86**(Suppl 3)**:**S734–S740.
10. Shetty AK, Steele RW, Silas V, Dehne R 1998 A boy with a limp. Lancet **351:**182.
11. Banhegyi G, Braun L, Csala M, Puskas F, Mandl J 1997 Ascor-

bate metabolism and its regulation in animals. Free Radic Biol Med **23:**793–803.

12. Ha MN, Graham FL, D'Souza CK, Muller WJ, Igdoura SA, Schellhorn HE 2004 Functional rescue of vitamin C synthesis deficiency in human cells using adenoviral-based expression of murine l-gulono-gamma-lactone oxidase. Genomics **83:**482–492.
13. Mahan DC, Ching S, Dabrowski K 2004 Developmental aspects and factors influencing the synthesis and status of ascorbic acid in the pig. Annu Rev Nutr **24:**79–103.
14. Nishikimi M, Fukuyama R, Minoshima S, Shimizu N, Yagi K 1994 Cloning and chromosomal mapping of the human nonfunctional gene for L-gulono-gamma-lactone oxidase, the enzyme for L-ascorbic acid biosynthesis missing in man. J Biol Chem **269:**13685–13688.
15. Nishikimi M, Yagi K 1991 Molecular basis for the deficiency in humans of gulonolactone oxidase, a key enzyme for ascorbic acid biosynthesis. Am J Clin Nutr **54**(6 Suppl)**:**1203S–1208S.
16. Mohan S, Richman C, Guo R, Amaar Y, Donahue LR, Wergedal J, Baylink DJ 2003 Insulin-like growth factor regulates peak bone mineral density in mice by both growth hormone-dependent and -independent mechanisms. Endocrinology **144:**929–936.
17. Kasukawa Y, Baylink DJ, Wergedal JE, Amaar Y, Srivastava AK, Guo R, Mohan S 2003 Lack of insulin-like growth factor I exaggerates the effect of calcium deficiency on bone accretion in mice. Endocrinology **144:**4682–4689.
18. Parfitt AM, Drezner MK, Glorieux FH, Kanis JA, Malluche H, Meunier PJ, Ott SM, Recker RR 1987 Bone histomorphometry: Standardization of nomenclature, symbols, and units. Report of the ASBMR Histomorphometry Nomenclature Committee. J Bone Miner Res **2:**595–610.
19. Richman C, Baylink DJ, Lang K, Dony C, Mohan S 1999 Recombinant human insulin-like growth factor-binding protein-5 stimulates bone formation parameters in vitro and in vivo. Endocrinology **140:**4699–4705.
20. Chung YS, Baylink DJ, Srivastava AK, Amaar Y, Tapia B, Kasukawa Y, Mohan S 2004 Effects of secreted frizzled-related protein 3 on osteoblasts in vitro. J Bone Miner Res **19:**1395–1402.
21. Takamizawa S, Maehata Y, Imai K, Senoo H, Sato S, Hata R 2004 Effects of ascorbic acid and ascorbic acid 2-phosphate, a long-acting vitamin C derivative, on the proliferation and differentiation of human osteoblast-like cells. Cell Biol Int **28:**255–265.
22. Franceschi RT, Iyer BS 1992 Relationship between collagen synthesis and expression of the osteoblast phenotype in MC3T3-E1 cells. J Bone Miner Res **7:**235–246.
23. Franceschi RT, Iyer BS, Cui Y 1994 Effects of ascorbic acid on collagen matrix formation and osteoblast differentiation in murine MC3T3-E1 cells. J Bone Miner Res **9:**843–854.
24. Akikusa JD, Garrick D, Nash MC 2003 Scurvy: Forgotten but not gone. J Paediatr Child Health **39:**75–77.
25. Pimentel L 2003 Scurvy: Historical review and current diagnostic approach. Am J Emerg Med **21:**328–332.
26. Hasan L, Vogeli P, Stoll P, Kramer SS, Stranzinger G, Neuenschwander S 2004 Intragenic deletion in the gene encoding L-gulonolactone oxidase causes vitamin C deficiency in pigs. Mamm Genome **15:**323–333.
27. Sakamoto Y, Takano Y 2002 Morphological influence of ascorbic acid deficiency on endochondral ossification in osteogenic disorder Shionogi rat. Anat Rec **268:**93–104.
28. Tsunenari T, Fukase M, Fujita T 1991 Bone histomorphometric analysis for the cause of osteopenia in vitamin C-deficient rat (ODS rat). Calcif Tissue Int **48:**18–27.
29. Kawai T, Nishikimi M, Ozawa T, Yagi K 1992 A missense mutation of L-gulono-gamma-lactone oxidase causes the inability of scurvy-prone osteogenic disorder rats to synthesize L-ascorbic acid. J Biol Chem **267:**21973–21976.
30. Maeda N, Hagihara H, Nakata Y, Hiller S, Wilder J, Reddick R 2000 Aortic wall damage in mice unable to synthesize ascorbic acid. Proc Natl Acad Sci USA **97:**841–846.
31. Zorzoli A, Nadel EM 1953 Alkaline phosphatase activity in the bones of normal and scorbutic guinea pigs; a correlated biochemical and histochemical study. J Histochem Cytochem **1:**362–371.
32. Chen TL, Raisz LG 1975 The effects of ascorbic acid deficiency on calcium and collagen metabolism in cultured fetal rat bones. Calcif Tissue Res **17:**113–127.
33. Franceschi RT, Young J 1990 Regulation of alkaline phosphatase by 1,25-dihydroxyvitamin D3 and ascorbic acid in bone-derived cells. J Bone Miner Res **5:**1157–1167.
34. Gerstenfeld LC, Chipman SD, Glowacki J, Lian JB 1987 Expression of differentiated function by mineralizing cultures of chicken osteoblasts. Dev Biol **122:**49–60.
35. Owen TA, Aronow M, Shalhoub V, Barone LM, Wilming L, Tassinari MS, Kennedy MB, Pockwinse S, Lian JB, Stein GS 1990 Progressive development of the rat osteoblast phenotype in vitro: Reciprocal relationships in expression of genes associated with osteoblast proliferation and differentiation during formation of the bone extracellular matrix. J Cell Physiol **143:**420–430.
36. Xiao G, Cui Y, Ducy P, Karsenty G, Franceschi RT 1997 Ascorbic acid-dependent activation of the osteocalcin promoter in MC3T3-E1 preosteoblasts: Requirement for collagen matrix synthesis and the presence of an intact OSE2 sequence. Mol Endocrinol **11:**1103–1113.
37. Franceschi RT 1992 The role of ascorbic acid in mesenchymal differentiation. Nutr Rev **50:**65–70.
38. Komarova SV, Ataullakhanov FI, Globus RK 2000 Bioenergetics and mitochondrial transmembrane potential during differentiation of cultured osteoblasts. Am J Physiol Cell Physiol **279:**C1220–C1229.
39. Oyamada I, Palka J, Schalk EM, Takeda K, Peterkofsky B 1990 Scorbutic and fasted guinea pig sera contain an insulin-like growth factor I-reversible inhibitor of proteoglycan and collagen synthesis in chick embryo chondrocytes and adult human skin fibroblasts. Arch Biochem Biophys **276:**85–93.
40. Aronow MA, Gerstenfeld LC, Owen TA, Tassinari MS, Stein GS, Lian JB 1990 Factors that promote progressive development of the osteoblast phenotype in cultured fetal rat calvaria cells. J Cell Physiol **143:**213–221.
41. Sudo H, Kodama HA, Amagai Y, Yamamoto S, Kasai S 1983 In vitro differentiation and calcification in a new clonal osteogenic cell line derived from newborn mouse calvaria. J Cell Biol **96:**191–198.
42. Sugimoto T, Nakada M, Fukase M, Imai Y, Kinoshita Y, Fujita T 1986 Effects of ascorbic acid on alkaline phosphatase activity and hormone responsiveness in the osteoblastic osteosarcoma cell line UMR-106. Calcif Tissue Int **39:**171–174.
43. Knaack D, Podleski T 1985 Ascorbic acid mediates acetylcholine receptor increase induced by brain extract on myogenic cells. Proc Natl Acad Sci USA **82:**575–579.
44. Leboy PS, Vaias L, Uschmann B, Golub E, Adams SL, Pacifici M 1989 Ascorbic acid induces alkaline phosphatase, type X collagen, and calcium deposition in cultured chick chondrocytes. J Biol Chem **264:**17281–17286.
45. Taylor SM, Jones PA 1979 Multiple new phenotypes induced in 10T1/2 and 3T3 cells treated with 5-azacytidine. Cell **17:**771–779.
46. Takahashi T, Lord B, Schulze PC, Fryer RM, Sarang SS, Gullans SR, Lee RT 2003 Ascorbic acid enhances differentiation of embryonic stem cells into cardiac myocytes. Circulation **107:**1912–1916.
47. Yu DH, Lee KH, Lee JY, Kim S, Shin DM, Kim JH, Lee YS, Lee YS, Oh SK, Moon SY, Lee SH, Lee YS 2004 Changes of gene expression profiles during neuronal differentiation of central nervous system precursors treated with ascorbic acid. J Neurosci Res **78:**29–37.

48. Hall SL, Greendale GA 1998 The relation of dietary vitamin C intake to bone mineral density: Results from the PEPI study. Calcif Tissue Int **63:**183–189.
49. Kaptoge S, Welch A, McTaggart A, Mulligan A, Dalzell N, Day NE, Bingham S, Khaw KT, Reeve J 2003 Effects of dietary nutrients and food groups on bone loss from the proximal femur in men and women in the 7th and 8th decades of age. Osteoporos Int **14:**418–428.
50. Schnitzler CM, Schnaid E, Macphail AP, Mesquita JM, Robson HJ 2005 Ascorbic acid deficiency, iron overload and alcohol abuse underlie the severe osteoporosis in black African patients with hip fractures—a bone histomorphometric study. Calcif Tissue Int **76:**79–89.

Address reprint requests to:
Subburaman Mohan, PhD
Departments of Medicine and Biochemistry
Loma Linda University
Musculoskeletal Disease Center
Jerry L. Pettis Memorial VA Medical Center
11201 Benton Street
Loma Linda, CA 92357, USA
E-mail: Subburaman.Mohan@med.va.gov

Received in original form February 2, 2005; revised form March 25, 2005; accepted April 15, 2005.